ISSN 1063-7745, Crystallography Reports, 2017, Vol. 62, No. 1, pp. 133–138. © Pleiades Publishing, Inc., 2017.
Original Russian Text © A.Kh. Abduev, A.K. Akhmedov, A.Sh. Asvarov, N.M.-R. Alikhanov, R.M. Emirov, A.E. Muslimov, V.V. Belyaev, 2017, published in Kristallografiya, 2017, Vol. 62, No. 1, pp. 130–136.

SURFACE AND THIN FILMS

Gas-phase Clusterization of Zinc during Magnetron Sputtering

A. Kh. Abduev[a], A. K. Akhmedov[a], A. Sh. Asvarov[a,b], N. M.-R. Alikhanov[c], R. M. Emirov[c], A. E. Muslimov[d], and V. V. Belyaev[e,*]

[a] *Institute of Physics, Dagestan Scientific Center, Russian Academy of Sciences, Makhachkala, Dagestan, 367003 Russia*
[b] *Dagestan Scientific Center, Russian Academy of Sciences, Analytical Center of Collective Use, Makhachkala, Dagestan, 367025 Russia*
[c] *Dagestan State University, Makhachkala, Dagestan, 367000 Russia*
[d] *Shubnikov Institute of Crystallography, Federal Scientific Research Centre "Crystallography and Photonics," Russian Academy of Sciences, Moscow, 119333 Russia*
[e] *Moscow Region State University, Moscow, 105005 Russia*
**e-mail: abil-as@list.ru*

Received May 19, 2016

Abstract—The processes of gas-phase clusterization of zinc during dc magnetron sputtering of a zinc target in an argon atmosphere have been investigated. The influence of the working gas pressure and magnetron discharge current on the morphology and structure of the precipitates formed on substrates previously cooled to −50°C is studied. It is shown that dense textured (002)Zn layers with a columnar structure are formed at relatively low argon pressures in the chamber ($P = 0.5$ Pa) and low discharge currents (100 mA). X-ray amorphous deposits with a fractal coral-like structure arise on substrates at an extremely high argon pressure in the chamber ($P = 5$ Pa). An increase in the magnetron discharge current at an operating gas pressure of *5* Pa leads to the formation of polycrystalline layers on substrates; the intensity of the XRD peaks related to crystalline zinc increases with an increase in the discharge current. Possible mechanisms of the structural transformation of Zn deposits are considered.

DOI: 10.1134/S1063774517010023

INTRODUCTION

The study of the formation of metal cluster layers during magnetron sputtering is one of the priority lines of research in condensed-matter physics. These processes include both gas-phase formation of clusters via diffusion-limited aggregation and subsequent formation of coatings during cluster–cluster aggregation [1, 2]. A number of reviews (see, e.g., [3]) have been devoted to the analysis of the gas-phase processes occurring in magnetron-discharge plasma, in their relationship with the formation of arrays of disordered structures on substrates.

Arrays of disordered structures with anomalously developed surface are also of great practical interest due to the possibility of using them to fabricate conducting layers for "transparent" electronics [4, 5] and active dye layers in solar energy converters [6] and gas sensors [7].

Plasma clusterization of vapors of various materials and subsequent formation of deposits with a fractal structure were observed previously, e.g., during electric-arc sputtering of ZnO [8] and interaction of thermonuclear plasma with the material of reactor walls [9].

The clusterization of the reagent flow formed as a result of magnetron sputtering is primarily caused by the relatively low temperature and high working pressure of gas, due to which the probability of collisions between sputtered atoms and molecules and their aggregation increases. The presence of clusters in the reagent flow significantly affects the structure and properties of layers [10].

In this paper, we report the results of studying the processes of gas-phase clusterization of zinc during magnetron sputtering of a Zn target and the dependence of the deposit structure on the working-gas pressure and sputtering rate. The deposition was performed onto a cooled substrate in order to reduce the influence of the substrate temperature on the structure of the deposited layers.

EXPERIMENTAL

Sputtering was performed in 99.999% purity argon. The sputtered target was a 99.95% purity zinc disk with a thickness of 3.5 mm and a diameter of 51 mm. The target–substrate distance was 60 mm in all experiments. The discharge current was varied from 100 to 300 mA. Borosilicate glass and silicon substrates with thermally oxidized surfaces were installed on a copper holder cooled by liquid nitrogen vapor. Layers were deposited on substrates cooled to −50°C. The argon

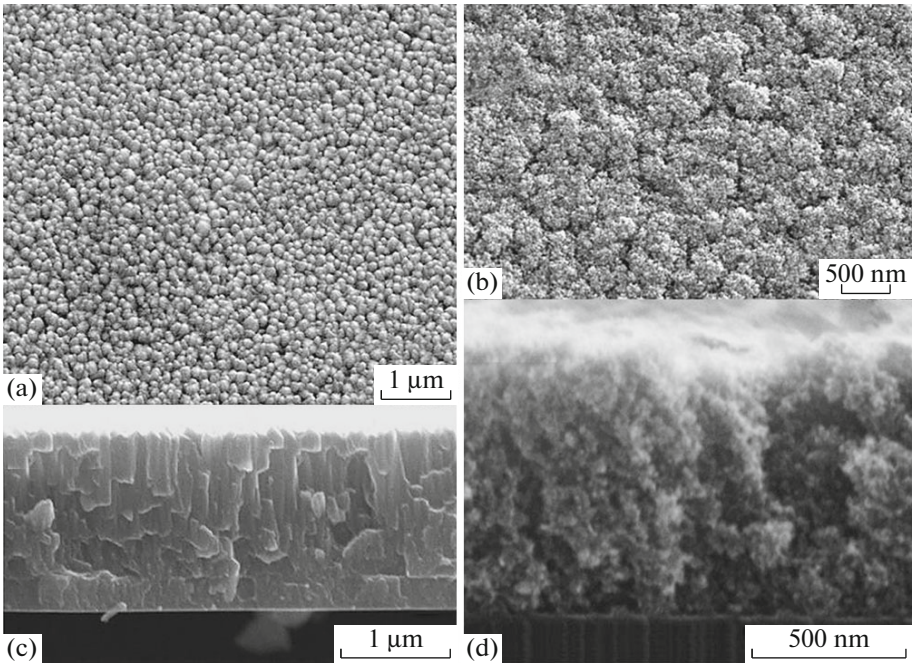

Fig. 1. Micrographs of the (a, b) surface and (c, d) cross-section of the zinc layers obtained at a discharge current of 100 mA and argon pressures of (a, c) 0.5 and (b, d) 5 Pa.

pressure was varied from 0.5 to 5 Pa in different experiments.

To reduce the influence of the desorption of gases adsorbed on the target surface on the stability of magnetron discharge current–voltage characteristics, the target was subjected to preliminary sputtering with a closed shutter for 5 min before each working cycle.

The deposited-layer morphology was studied using a Leo-1450 scanning electron microscope (Carl Zeiss, Germany). X-ray diffraction analysis was carried out with an Empyrean diffractometer (PANalytical B.V., Netherlands). Diffraction patterns were recorded under the following conditions: standard (Bragg–Brentano) beam focusing geometry, tube voltage U = 40 kV, tube current I = 30 mA, X-ray wavelength $\lambda_{CuK\alpha}$ = 1.5406 Å, nickel filter in the primary beam, $\theta-2\theta$ scan mode, scan range 25°–78°, scan step 0.013°, exposure time per point 120 s, and temperature T = 25°C. The experimental data were processed using the HighScore Plus software.

RESULTS

We investigated the processes occurring in the gas phase and the structure of the layers deposited during magnetron sputtering of zinc target in two different modes: at low Ar pressures (in order to minimize the interaction between sputtered atoms in the gas phase) and at the highest (maximally possible) Ar pressures in the chamber (to study the aggregation of sputtering products in the gas phase).

At a low working gas pressure (P_{Ar} = 0.5 Pa), dense smooth layers of silverish white color are formed on substrates. The layers synthesized at P_{Ar} = 1 Pa have a gray dull surface. The synthesis under an extremely high pressure (P_{Ar} = 5 Pa) provides weakly reflecting layers of black color, which is indicative of their large specific surface area [11]. With an increase in the argon pressure, the layer growth rate monotonically decreases from 172 nm/min for P_{Ar} = 0.5 Pa to 90 nm/min for P_{Ar} = 5 Pa.

Micrographs of the surface and cross-section of the layers synthesized at a discharge current of 100 mA and argon pressures of 0.5 and 5 Pa are shown in Fig. 1. One can see that the layer synthesized at P_{Ar} = 0.5 Pa has a pronounced columnar structure (Figs. 1a, 1c), which is characteristic for the layers synthesized from an atomic flux under far-from-equilibrium conditions. Apparently, at low working gas pressures, zinc mostly arrives at the growth surface in the form of atoms. Note that, even at a substrate temperature of −50°C, zinc atoms can still migrate over the growth surface to form dense polycrystalline layers [12].

A study of the deposits formed on the substrate at a high argon pressure (P_{Ar} = 5 Pa) showed that the deposited layers have a developed surface morphology with signs of fractal structure (Fig. 1b). An analysis of the surface of the layers with high magnifications revealed that the minimum size of resolved objects in the micrograph is about 20 nm. The micrograph of the cross-section view of this sample (Fig. 1d) demonstrates a loose coral-like structure, which is character-

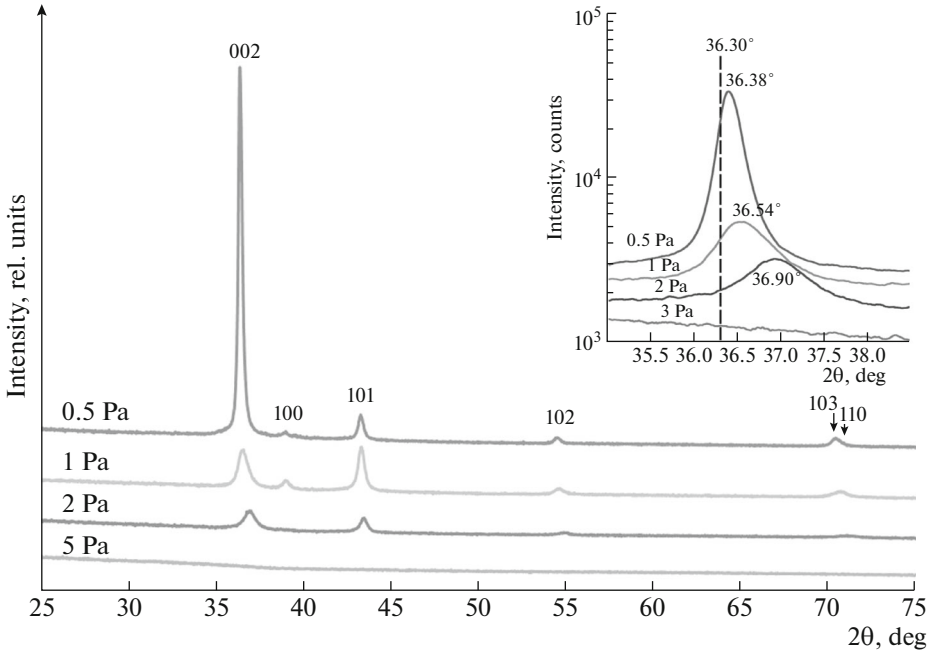

Fig. 2. X-ray diffraction patterns of the Zn layers deposited on glass substrates at a discharge current I_{dis} = 100 mA and different argon pressures. The inset shows the displacement and change in the profile of the 002 peak with an increase in argon pressure in the chamber.

istic for the layers formed from cluster fluxes at a close-to-zero migration rate of clusters on the growth surface.

The X-ray diffraction spectra of the layers synthesized at different working gas pressures and a fixed discharge current (100 mA) are presented in Fig. 2. One can see that a textured polycrystalline Zn film with a hexagonal structure and preferred orientation of the *c* axis along the normal to the growth surface is formed at minimal pressures. An increase in pressure reduces both the crystallinity and the degree of preferred orientation of layers, up to their complete amorphization at P_{Ar} = 5 Pa. The inset in Fig. 2 shows the transformation of the 002 Zn peak with an increase in pressure in the chamber. It is important that, in contrast to the observable significant shift of the 002 peak to larger 2θ angles with an increase in pressure P_{Ar}, the shift of the other peaks was either zero or small.

To determine the temperature stability of the aggregates formed in the gas phase at P_{Ar} = 5 Pa, we additionally investigated the formation of coatings at this pressure and their microstructure in dependence of the magnetron discharge current. The increase in the discharge current at a fixed working gas pressure is expectedly accompanied by an increase in the layer growth rate from 90 to 135 nm/min. At the same time, the zinc layers obtained at P_{Ar} = 5 Pa remain black with an increase in discharge current I_{dis} from 100 to 300 mA; however, their smoothness visually increases, a fact indicating compaction of their structure.

Micrographs of the surface and cross-section of the layer synthesized at P_{Ar} = 5 Pa and discharge current I_{dis} = 300 mA are presented in Fig. 3. One can see that the structure of the surface and cross-section of layer is intermediate between the loose coral-like structure of the deposits formed at discharge current I_{dis} = 100 mA and pressure P_{Ar} = 5 Pa (Figs. 1b, 1d) and the dense columnar structure of the layers grown at P_{Ar} = 0.5 Pa (Figs. 1a, 1c). Individual grains up to 50 nm in size can be discerned on the surface; some of them form convex agglomerates up to 500 nm in diameter (indicated by an arrow in Fig. 3a). Both individual grains and columnar aggregates of irregular shape are observed in the cross-section view micrograph.

Figure 4 shows an X-ray diffraction pattern of the Zn layers formed at P_{Ar} = 5 Pa and different discharge currents I_{dis}. One can see that the increase in the discharge current is accompanied by the inverse transition from the X-ray amorphous phase to the polycrystalline phase. The 101 Zn peak arises in the X-ray diffraction pattern at I_{dis} = 180 mA, and a further increase in the discharge current to 300 mA gives rise to peaks corresponding to other orientations of Zn nanocrystallites. The polycrystalline sample obtained at the maximum discharge current is characterized by different widths of reflections. The 002 Zn peak is much wider than the two neighboring 100 and 101 Zn peaks. Note also the pronounced asymmetry of the strongest 002 and 101 peaks. The observed difference in the peak width may be related both to the difference in the

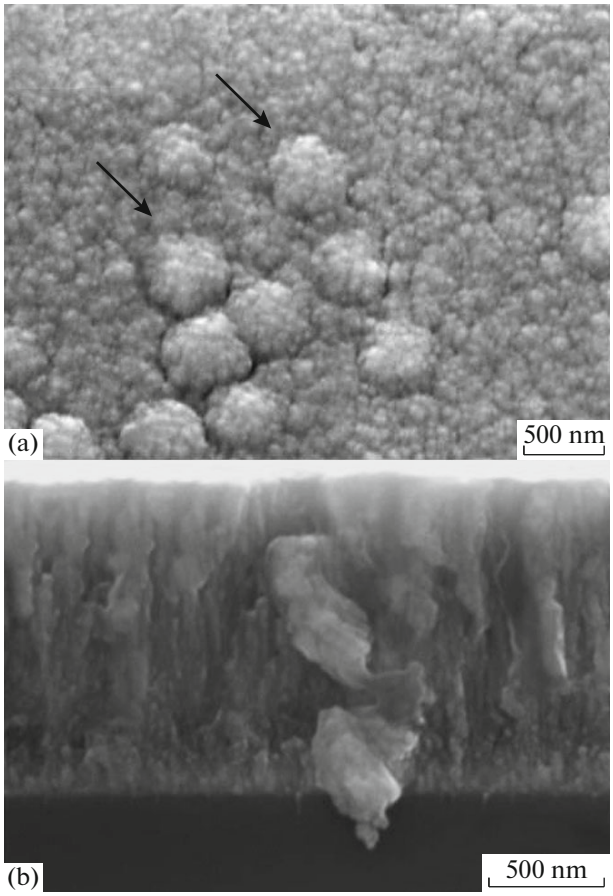

Fig. 3. Micrographs of the (a) surface and (b) cross-section of the zinc layers obtained at an argon pressure of 5 Pa and a discharge current of 300 mA.

sizes of Zn crystallites with different orientation of the *c* axis and to the difference in their microdistortions [13, 14]. The asymmetric profile of the Zn peaks may indicate the presence of several types of Zn nanocrystallites with differing interplanar spacings d_{hkl} in the film (the inset in Fig. 4 shows as an example a decomposition of the profiles of the 002 and 101 peaks into two components).

Lattice parameters *a* and *c* and average crystallite size D_{002} for the Zn layers synthesized at different pressures P_{Ar} and magnetron discharge currents I_{dis}

P_{Ar}, Pa	I_{dis}, mA	*c*, nm	*a*, nm	*c*/*a*	D_{002}, nm
0.5	100	0.4934	0.2666	1.8507	41.3
1	100	0.4912	0.2666	1.8425	15.6
2	100	0.4866	0.2664	1.8266	10.3
5	100	X-ray amorphous phase			
5	300	⟨0.4836⟩	0.2664	⟨1.8153⟩	8.0

The tabulated values of bulk zinc lattice parameters $c = 0.49450$ nm, $a = 0.26650$ nm, $c/a = 1.8556$ are taken from the inorganic crystal structure database (ICSD pattern: 98-005-2259, PDF code: 00-004-0831).

Based on the X-ray diffraction data collected for all samples, we calculated unit-cell parameters *c* and *a*. In addition, using the features of the 002 Zn peak, we calculated the average crystallite sizes D_{002} from the Selyakov–Scherrer formula. The table contains generalized data on the structural characteristics of Zn layers synthesized at different argon pressures and magnetron discharge currents.

The data listed in the table indicate that the polycrystalline Zn layers synthesized at a low discharge current (I_{dis} = 100 mA) and minimal pressure in the chamber (P_{Ar} = 0.5 Pa) consist of Zn nanocrystallites with an average size D_{002} = 41.3 nm, the *c* axis of which is mainly oriented along the normal to the surface. Lattice parameters *c* and *a* of these crystallites are close to the tabulated values for bulk zinc.

An increase in the working gas pressure in the chamber to 2 Pa leads to a decrease in the average size of nanocrystallites to D_{002} = 10.3 nm, their misorientation, and reduction of the *c*/*a* ratio to 1.8266 due to the decrease in parameter *c*, with parameter *a* remaining constant. At P_{Ar} = 5 Pa, Zn deposits become completely X-ray amorphous.

However, the increase in the discharge current to 300 mA at P_{Ar} = 5 Pa leads to the formation of Zn layers containing not only X-ray amorphous but also nanocrystalline phase with an average crystallite size smaller than 10 nm, where the *c*/*a* ratio is also much smaller than the tabulated value.

DISCUSSION

The bombardment of a metal target with argon ions leads to efficient emission of high-energy Zn atoms (with an energy of about 9 eV [3]) from its surface. In addition, bombardment causes heating of a thin surface layer of the target to a temperature ~0.7 T_m, due to which additional thermal emission of zinc atoms with lower energy may occur. Thus, a flux of zinc atoms directed from the target to the substrate is formed directly after the narrow near-cathode plasma region. The flow density of zinc atoms and the thermalization and isotropization times depend strongly on the working gas pressure. An increase in pressure (i.e., increase in the density of scattering centers—inert-gas atoms) reduces the mean free path of sputtered atoms and increases the probability of forming zinc clusters in the gas phase due to the three-particle formation of a nucleus in the form of a diatomic molecule ($2Zn + Ar \rightarrow Zn_2 + Ar$) and its subsequent growth ($Zn_n + Zn \rightarrow Zn_{n+1}$). Thus, at a discharge current of 100 mA and the pressure in the chamber increased to 5 Pa, zinc clusters can be formed in the gas phase under the conditions of limited atomic diffusion [11, 15]. Layers are formed from a flux containing both atomic and cluster components. An increase in pressure leads to a decrease in the atomic component in the flux and, correspondingly, an increase in

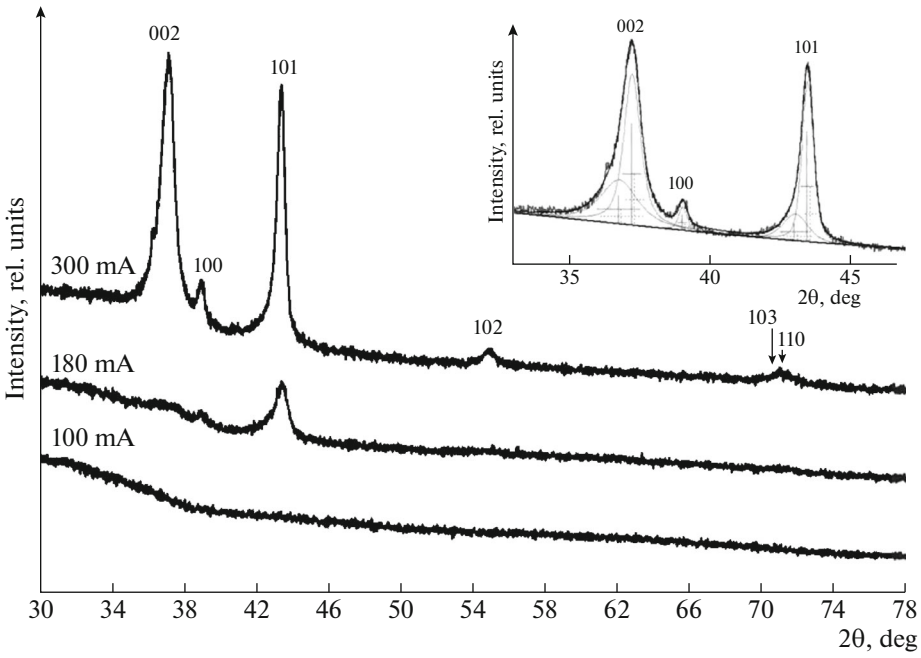

Fig. 4. X-ray diffraction patterns of the layers synthesized at an argon pressure of 5 Pa and different magnetron discharge currents. The inset shows a fragment of the X-ray diffraction pattern of the Zn layer synthesized at I_{dis} = 300 mA and the result of decomposition of the 002 and 101 reflections into two components.

the cluster flux density. The crystalline Zn phase in the growing layer is formed by Zn adatoms with nonzero migration ability, while the X-ray amorphous phase is formed by disordered Zn clusters incorporated into the layer according to the mechanism of cluster–cluster aggregation. It is reasonable to suggest that, under maximum pressure, the loose black X-ray amorphous layer with a coral-like structure is formed mainly by disordered Zn clusters. The observed decrease in the average size of Zn nanocrystallites with an increase in working gas pressure can be explained by the decrease in both the flow density of zinc atoms near the growth surface and their migration ability because of the elevated concentration of argon atoms and Zn clusters.

One would explain the unusual behavior of the unit-cell parameters with a decrease in the average size of Zn nanocrystallites (decrease in parameter *c* with invariable parameter *a*) by the size effect. However, it was clearly shown in [13]] that this behavior of the lattice parameters of the zinc layers formed by dc magnetron sputtering under intense ion bombardment of the growth surface correlates well with the content of argon incorporated into the film (buried in it). A relationship between the peak profile asymmetry and the gradient of argon content throughout the film thickness was also noted in [13]. Since the decrease in the crystallite size and the peak asymmetry are observed at an Ar pressure increased by an order of magnitude, the relationship between the observed decrease in parameter *c* and the content of incorporated argon looks quite logical. However, clarification of the mechanism of argon incorporation into the growing Zn film and its influence on the film microstructure undoubtedly calls for a more detailed study.

The occurrence of crystalline phase in the Zn films deposited under the conditions favorable for gas-phase cluster formation (P_{Ar} = 5 Pa) with an increase in the magnetron discharge current can be explained by the increase in the particle temperature in the magnetron discharge plasma and the corresponding increase in the fraction of atomic zinc in the reagent flux.

First, an increase in the particle temperature in the magnetron discharge plasma may lead to thermal decomposition of clusters. Clusters in magnetron discharge are heated when metal atoms are attached to them. According to the estimates reported in [3], the cluster temperature during magnetron sputtering may reach several hundreds of Celsius degrees, i.e., values greatly exceeding the working gas temperature. This, in turn, leads to evaporation of zinc atoms from the cluster surface. The evaporation of Zn clusters increases the fraction of atomic zinc in the reagent flux, which improves the crystallinity of deposited layers.

Second, heating of the working gas reduces its density, i.e., decreases the number of scattering centers and, correspondingly, increases the thermalization time and mean free path of sputtered zinc atoms [16]. Thus, the probability for the nonclustered material to reach the substrate increases.

Third, despite the intense cooling of the substrate from the side of the holder, one must take into account

the increase in the thermal load on the growth surface due to the radiation, which, in turn, may lead to partial thermal decomposition of clusters on the substrate and increase the migration ability of zinc adatoms.

CONCLUSIONS

The processes of gas-phase clusterization of zinc vapor can be either initiated or suppressed during magnetron sputtering of a metallic zinc target, depending on the working gas pressure and the discharge current in magnetron plasma.

At a pressure of 0.5 Pa in the chamber, the efficiency of zinc vapor clusterization in the gas phase is minimal, and dense polycrystalline zinc layers with a columnar structure are formed on the substrate surface at a temperature of −50°C. An increase in the argon pressure reduces the layer crystallinity due to the presence of fractal cluster structures (formed in the gas phase) in the reagent flux. At the maximum argon pressure (P_{Ar} = 5 Pa), coral-like amorphous arrays of disordered structures with an anomalously developed surface are deposited on substrates; they may be of independent interest for various device applications. These structures are formed according to the mechanism of cluster–cluster aggregation.

An increase in the discharge current leads to the thermal decomposition of fractal aggregates and increase in the atomic zinc fraction in the reagent flux. As a result, the deposition occurs under conditions of high zinc vapor pressure above the growth surface, as a result of which the degree of crystallinity of the layers increases.

ACKNOWLEDGMENTS

This study was performed using the equipment of the Analytical Collective-Use Center of the Dagestan Scientific Center, Russian Academy of Sciences, and supported by the Russian Foundation for Basic Research, project nos. 16-07-00469 and 16-07-00503.

REFERENCES

1. T. A. Witten and I. M. Sander, Phys. Rev. Lett. **47**, 1400 (1981).
2. S. A. Beznosyuk, Ya. V. Lerkh, and T. M. Zhukhovitskaya, Polzunovskii Vestn. **41**, 143 (2005).
3. P. V. Kashtanov, B. M. Smirnov, and R. Hippler, Phys. Usp. **50**, 455 (2007).
4. A. Lamberti, A. Sacco, M. Laurenti, et al., J. Alloys Compd. **615**, S487 (2013).
5. A. Abduev, A. Akhmedov, A. Asvarov, and A. Chiolerio, Plasma Processes Polym. **12**, 725 (2015).
6. A. Hagfeldt, G. Boschloo, L. Sun, et al., Chem. Rev. **110**, 6595 (2010).
7. A. Wei, L. Pan, and W. Huang, Mater. Sci. Eng. B **176**, 1409 (2011).
8. A. Kh. Abduev, A. Sh. Asvarov, A. K. Akhmedov, et al., Tech. Phys. Lett. **28**, 952 (2002).
9. V. P. Budaev and L. N. Khimchenko, JETP **104**, 629 (2007).
10. A. Kh. Abduev, A. M. Magomedov, and Sh. O. Shakhshaev, Neorg. Mater. **33**, 340 (1997).
11. H. Levinstein, J. Appl. Phys. **20**, 306 (1949).
12. J. A. Thornton, Ann. Rev. Mater. Sci. **7**, 239 (1977).
13. R. Kuiel, V. Valvoda, M. Chladek, et al., Thin Solid Films **263**, 150 (1995).
14. Ch. Taviot-Guého, J. Cellier, A. Bousquet, and E. Tomasella, J. Phys. Chem. C **119**, 23559 (2015).
15. A. G. Znamenskii and V. A. Marchenko, Tech. Phys. **43**, 66 (1998).
16. S. M. Rossnagel, IEEE Trans. Plasma Sci. **18**, 878 (1990).

Translated by Yu. Sin'kov